

Heat contribution of the Indonesian throughflow to the Indian Ocean

Tiecheng Zhang^{1,3}, Weiqiang Wang^{2,4}, Qiang Xie^{1,2,4*}, Lingfang Chen¹

¹ Institute of Deep-sea Science and Engineering, Chinese Academy of Sciences, Sanya 572000, China

² State Key Laboratory of Tropical Oceanography, South China Sea Institute of Oceanology, Chinese Academy of Sciences, Guangzhou 510301, China

³ University of Chinese Academy of Sciences, Beijing 100049, China

⁴ Laboratory for Regional Oceanography and Numerical Modeling, Pilot National Laboratory for Marine Science and Technology (Qingdao), Qingdao 266237, China

Received 8 February 2018; accepted 27 April 2018

© Chinese Society for Oceanography and Springer-Verlag GmbH Germany, part of Springer Nature 2019

Abstract

Based on the high-resolution Eulerian fields of an ocean general circulation model simulation, the heat contribution of the Indonesian throughflow (ITF) to the Indian Ocean is estimated by Lagrangian tracing method. The heat transport of each particle of ITF waters is calculated by tracing temperature change along the trajectory until the particle exits the Indian Ocean. The simulation reveals that the ITF waters flow westward and branch near Madagascar, further showing the ITF waters are redistributed in both northern and southern Indian Ocean. Heat budget analysis indicates that the ITF waters gain 0.41 PW (Petawatts, 10^{15} W) in the northern Indian Ocean and lose 0.56 PW in the southern Indian Ocean, respectively. As a result, the ITF waters warm the whole Indian Ocean basin with only 0.15 PW, which shows an “insignificant” role of ITF on the Indian Ocean because of the heat exchange compensation between northern and southern Indian Ocean. Furthermore, the tracing pathways show that the ITF waters mainly flow out the Indian Ocean at both sides of the basin via Agulhas Current and Leeuwin Current. About 89% of the ITF waters leave along western boundary and the rest 11% along eastern boundary. Compared to seeding section, 0.10 PW and 0.05 PW are released to the Indian Ocean, respectively.

Key words: Indonesian throughflow, Indian Ocean, heat contribution

Citation: Zhang Tiecheng, Wang Weiqiang, Xie Qiang, Chen Lingfang. 2019. Heat contribution of the Indonesian throughflow to the Indian Ocean. *Acta Oceanologica Sinica*, 38(4): 72–79, doi: 10.1007/s13131-019-1414-6

1 Introduction

The Indonesian throughflow (ITF) is a vital component of the Global Conveyor Belt, and plays an important role in the global ocean and climate regulation (Gordon, 1986; Godfrey, 1996). The ITF carries warm and fresh tropical waters from the Pacific into the Indian Ocean, which strongly influences the state of the Pacific Ocean and Indian Ocean and modulates climate variability on a variety of time scales (Godfrey, 1996; Lee et al., 2002; McCreary et al., 2007; Song et al., 2007; Sprintall et al., 2014; Kajtar et al., 2015). The ITF is considered central to the heat and freshwater budgets of the Pacific Ocean and Indian Ocean (Vranes et al., 2002; Wajsowicz, 2002; Talley, 2003, 2008; Lumpkin and Speer, 2007; Macdonald and Baringer, 2013).

The spreading pathways of the ITF waters in the Indian Ocean are estimated in earlier studies. Most of the ITF waters are advected westward within the South Equatorial Current (SEC) between 10°S and 20°S (Gordon, 2005). The Lagrangian trajectory experiments show that at the western boundary about 38%±5% thermocline ITF waters flow southward to join the Agulhas Current, consequently exiting the Indian Ocean; the rest,

about 62%±5%, flow northward to the north of SEC (Song et al., 2004). The primary spreading pathway of the thermocline ITF water north of SEC is upwelling to the surface layer with subsequent advection southward within the surface Ekman layer toward the southern Indian Ocean subtropics (Song et al., 2004; Valsala and Ikeda, 2007). Most of the ITF waters leave the Indian Ocean within the Agulhas Current (AC) (Haines et al., 1999; Song et al., 2004). There are also a portion of the ITF waters feeding the Leeuwin Current (LC), which are assessed in detail by Domingues et al. (2007) and Seville et al. (2014).

Much attention has been paid to the net heat contribution of ITF to the Indian Ocean. ITF heat flux into the Indian Ocean is estimated about 0.5 to 1.4 PW (Petawatts, 10^{15} W), depending on ITF volume transport and reference temperature (Vranes et al., 2002; Talley, 2003; Lumpkin and Speer, 2007; Macdonald and Baringer, 2013). The reference temperature 0°C is often chosen out of simplicity (Talley, 2003; Macdonald and Baringer, 2013). The ITF waters eventually exit the Indian Ocean across 34°S (Haines et al., 1999; Song et al., 2004; Valsala and Ikeda, 2007). After a reasonable reference temperature for ITF exiting the Indi-

Foundation item: The Strategic Priority Research Program of Chinese Academy of Sciences under contract Nos XDA20060502 and XDA11010301; the National Key Research and Development Program of China under contract No. 2016YFC1401401; the National Natural Science Foundation of China under contract Nos 41676013, 41521005 and 41731173; the Independent Research Project Program of State Key Laboratory of Tropical Oceanography under contract No. LTOZZ1702; the CAS/SAFEA International Partnership Program for Creative Research Teams.

*Corresponding author, E-mail: gordonxie@idsse.ac.cn

an Ocean is chosen, the ITF heat flux on the Indian Ocean can be estimated. Based on direct mooring measurements in the Makassar Strait and AC region, Vranes et al. (2002) estimate the ITF heat flux under various scenarios, concluding that the net heat contribution of ITF to the Indian Ocean is insignificant. This result is consistent with the estimations of the divergence of temperature fluxes between the Indonesian seas and the southern boundary of the Indian Ocean by other studies (Banks, 2000; Talley, 2003; Macdonald and Baringer, 2013).

An open question is therefore raised that whether the ITF warms or cools the Indian Ocean. Gordon (2005) argues that the ITF cools the Indian Ocean. Due to that the thermocline of the Indonesian seas is colder than that of the Indian Ocean. He assumes that the warm tropical and northern Indian Ocean thermocline would close in and fill the void if there were no ITF. On the contrary, by contrasting a control model run with a “closed ITF” run, many model experiments conclude that the ITF warms the Indian Ocean (Lee et al., 2002; Song et al., 2007; Kajtar et al., 2015). When ITF passages are closed, sea surface temperature in the southern Indian Ocean gets cooler and the mean thermocline shoals in the Indian Ocean. However, it is worth noting that “anomaly” fields between experiments open and closed ITF should be treated with caution because it is not clear whether such a climate state resulting from a closed ITF is realizable (Gordon, 2005). The initial and boundary conditions for closed ITF usually are set to the same as that for open one, which is often unreasonable but hard to solve because that we even do not know what the reasonable conditions should be. Besides, the difference induced by closed ITF is may contaminated by the numerical errors as well (Valsala and Ikeda, 2007).

In the present study we will pay our attention to quantitatively estimate the heat contribution of the ITF waters to the Indian Ocean. The spreading pathways and temperature change of the ITF waters in the Indian Ocean are examined, using Lagrangian method based on the high-resolution Eulerian fields. The rest of the paper is organized as follows. The data and methods are introduced in Section 2, the results are presented in Section 3, followed by the conclusions and discussion in Section 4.

2 Data and methods

2.1 Model data

The high-resolution ocean general circulation model for the earth simulator (OFES) output (Masumoto et al., 2004) is used in this study. This model is a quasi-global (75°N–75°S), with horizontal resolution of 0.1° and 54 levels in the vertical direction. The vertical grid spacing varies from 5 m in the upper levels to 330 m near the bottom with 20 levels confined in the upper 200 m to represent upper ocean circulation realistically. It was run for 50 years and the output, monthly mean climatological three-dimensional temperature, salinity and velocity fields for the last ten years (Years 41–50) is used in this analysis (see Masumoto et al. (2004) for more details).

The OFES data have been widely used to describe the ocean general circulation and the volume transport in the world oceans (Masumoto et al., 2004, 2008; Masumoto, 2010). In Indian Ocean, the Wyrtki Jets, Somali current system and Agulhas current system, main flows of the Indian Ocean, are well reproduced in the OFES data (Masumoto et al., 2004). Comparing with other ocean general circulation models, the OFES data is superior in simulating the meridional heat transport in the tropical Indian Ocean (Godfrey et al., 2007; Hu and Godfrey, 2007). The total ITF in OFES solution is about $11.6 \times 10^6 \text{ m}^3/\text{s}$ (Masumoto et al., 2004),

which is consistent with other ocean data assimilation products (Lee et al., 2010; Wang et al., 2010; Metzger et al., 2010), but larger than the earlier observations of about $10.6 \times 10^6 \text{ m}^3/\text{s}$ (Sprintall et al., 2004) and smaller than the recent observations of about $15 \times 10^6 \text{ m}^3/\text{s}$ (Gordon et al., 2010).

2.2 Tracing code and configurations

The TRACMASS code is used in this study to calculate Lagrangian trajectories from Eulerian velocity fields (Döös et al., 2013). The code computes numerically the trajectory through each grid cell by solving a differential equation that depends on the mass fluxes on the grid box walls. Each trajectory is associated with a certain volume transport given by the initial velocity and area. Due to the mass conservation of the TRACMASS schemes, mass transports can be calculated by summing over a set of trajectories between specific initial and final sections.

In the present study, ITF waters are traced from entering Indian Ocean to exiting Indian Ocean. Simulated parcels are initiated through all levels along the 8°S section on zonal-vertical plane to capture ITF waters into the Indian Ocean. One trajectory is initiated in each grid box, accounting for the transport across that grid box. The particles are released monthly over the first one year to account for seasonal variations. The trajectories are time dependent in the sense that the velocity fields are monthly updated during the integration, using the OFES output. At each time step, temperature, salinity, and density of the particles are all interpolated in time and space. In the present paper, the temperature variable we use is the potential temperature. Note that the ITF waters are mixed with the Indian Ocean waters and may change their properties. Hereafter we still dictate the modified waters during the journey as the ITF waters for convenient. These particles are tracked of 1 000 years or until they exit the Indian Ocean domain through southern boundary (34°S section). After 1 000 years, more than 99% of the particles exit the Indian Ocean, which indicates that 1 000 years should be enough to cover the ITF transport in the Indian Ocean.

2.3 Lagrangian diagnostic method

To examine where trajectories change their temperature, the Lagrangian divergence of heat flux is defined. Following Berglund et al. (2017), the tracer equation for temperature is approximated as

$$\nabla \cdot VT = D_T + Q, \quad (1)$$

where V is the three-dimensional velocity, D_T is the diffusion of temperature, and Q is the heat exchange, changing the temperature of the ocean. Here an incompressible flow ($\nabla \cdot V = 0$) is assumed and the long time means, over the considered time period, of the local rate of change ($\partial T / \partial t$) are negligible compared to the rate of change due to advection ($\nabla \cdot VT$). Further integrating Eq. (1) from the bottom to the surface and then multiplying with the heat capacity (taken as constant $4\,000 \text{ J}/(\text{K} \cdot \text{kg})$) and density of sea water (taken as constant $1\,025 \text{ kg}/\text{m}^3$, mean density of the ITF waters), the Lagrangian divergence of heat flux in a water column is obtained (see details in Berglund et al. (2017)).

The Lagrangian meridional streamfunction in latitude-temperature coordinates is used to diagnose the meridional heat transport. Following Döös et al. (2012) and Zika et al. (2012), it is defined as

$$\Psi_{Tj} = \sum_{i,k,n|T' \leq T} T_{i,j,k,n}^y, \quad (2)$$

where Ψ_{Tj} is the Lagrangian meridional stream function, $T_{i,j,k,n}^y$ is trajectory-derived volume transports in the meridional direction, and (i, j, k) represent grid indices in the x (zonal), y (meridional), and z (vertical) direction, respectively, where n represents the trajectory. It displays the northward volume transport across that part of the vertical surface at a specified latitude where the temperature T' is less than T . This is equal to the volume transport through the isothermal surface T north of the specified latitude in a statistically steady state (Döös et al., 2012). At 8°S section, since trajectories start there and the volume transport at this section is divergent, the streamfunction cannot be defined there.

Similarly, the Lagrangian meridional streamfunction in latitude-depth coordinates is defined as

$$\Psi_{j,k} = \sum_{\text{bottom}}^k \sum_i \sum_n T_{i,j,k,n}^y, \quad (3)$$

where $\Psi_{j,k}$ is the Lagrangian meridional streamfunction. The streamfunction corresponds to the mass flux integrated from the bottom to surface.

By calculating the heat entering, exiting, and loss-gain for each specific water mass, the heat exchanges between the entrance and the exit can be quantified. Following Koch-Larrouy et al. (2008), the heat transport for each trajectory is calculated as

$$H_{\text{in}} = \rho_0 c_p T_{\text{in}} t_r, \quad (4)$$

$$H_{\text{out}} = \rho_0 c_p T_{\text{out}} t_r, \quad (5)$$

$$H_{\text{net}} = \rho_0 c_p (T_{\text{in}} - T_{\text{out}}) t_r, \quad (6)$$

where H_{in} , H_{out} and H_{net} is the heat entering the Indian Ocean, exiting the Indian Ocean and the net heat loss-gain respectively, ρ_0 is the density of sea water ($1\,025\text{ kg/m}^3$), c_p is the specific heat of sea water ($4\,000\text{ J/(K}\cdot\text{kg)}$), t_r is the infinitesimal transport of the

trajectories considered, and T_{in} is temperature at the entrance section, and T_{out} at the exit section. Note that reference temperature for H_{in} and H_{out} is set to 0°C here, while H_{net} is independent on the reference temperature.

3 Results

In this section, we firstly depict transport pathways of the ITF waters in the Indian Ocean according to where the particles turn southward and exit the Indian Ocean. Then the heat contribution of the ITF waters to the Indian Ocean during their journey and the corresponding dynamic process is investigated. Finally the net heat contribution of the ITF waters to the whole Indian Ocean according to where the particles exit the Indian Ocean is further assessed in detail.

3.1 Typical routes

The ITF carries about $11.6 \times 10^6\text{ m}^3/\text{s}$ at around $8^\circ\text{--}22^\circ\text{S}$ from the Pacific into the Indian Ocean. The ITF waters flow westward and mostly join the SEC before reaching the Africa coast. When they close to the east coast of Madagascar, there are several routes for the ITF waters afterward. In order to examine the detail how the ITF waters interact with the Indian Ocean, the typical routes of the ITF transport are studied in the following.

There are several statistically significant routes of the ITF waters are shown in Fig. 1, which provides a straightforward way to see how the ITF waters spread in the Indian Ocean. These are (1) flowing southward at mouth of Indonesian archipelago and along Australia coast to feed the LC (Fig. 1a), (2) flowing along east coast of Madagascar after striding across the basin (Fig. 1b), (3) flowing through Mozambique Channel after striding across the basin (Fig. 1c), and (4) striding across the basin and flowing northward into northern Indian Ocean through western boundary current, and eventually leaving the southern Indian Ocean after circling in the northern Indian Ocean (Fig. 1d). These routes are hereafter denoted as Routes 1, 2, 3 and 4.

Different from other routes, Route 1 does not stride the

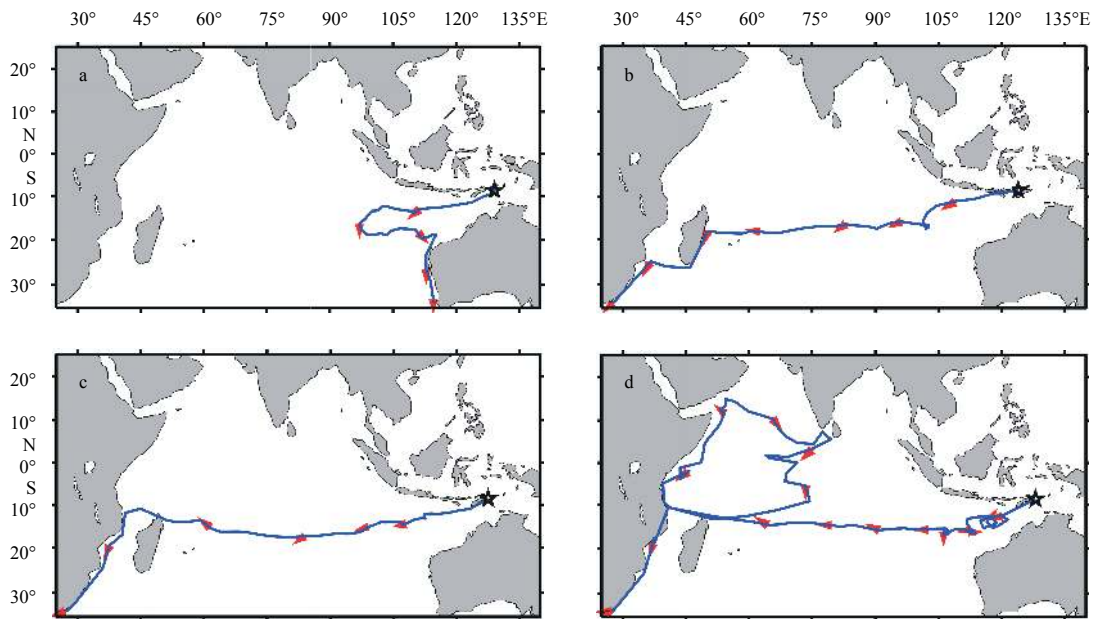


Fig. 1. A selection of illustrative trajectories according to where the particles turn southward and exit the Indian Ocean. ITF have four distinct routes: Route 1 (a), Route 2 (b), Route 3 (c), and Route 4 (d). The trajectories are projected on the horizontal plane, represented by blue curve. Black asterisk represents the initial position and red arrow the local transporting direction.

basins. It firstly flows to the west within SEC and then retroflexes into the Eastern Gyral Current. Afterward, it transits the Australian North-West Shelf in a surface poleward boundary flow and then exits the Indian Ocean within LC (Fig. 1a). The route agrees well with the simulated Lagrangian pathways by Domingues et al. (2007) carrying with about 11% ITF waters. Route 2 flows to the west within SEC until reaching east coast of Madagascar, turns southward into the Southeast Madagascar Current, and then exits the Indian Ocean within AC (Fig. 1b). Route 3 flows to the west within SEC until reaching east coast of Africa, turns southward into the Mozambique Channel, and then exits the Indian Ocean within AC (Fig. 1c). Route 4 flows to the west within SEC but then turns northward into the northern Indian Ocean along western boundary current (Fig. 1d). It consists of an important part of shallow meridional overturning circulation resulting in cold northward transport in subsurface and warm southward returning transport in surface (Valsala and Ikeda, 2007). Specifically, there are more than 50% of ITF waters carried by Route 4, which suggests there is a significant heat exchange process between ITF and the northern Indian Ocean.

3.2 Heat contribution of ITF to the Indian Ocean during the journey

It is quite surprising that the ITF would import a large amount of heat into the Indian Ocean without losing that heat while residing within the Indian Ocean (Vranes et al., 2002). This confusion drives us to investigate the heat contribution of ITF to the Indian Ocean during the journey, which is detailed in this subsection.

The Lagrangian divergence of heat flux for the ITF transport in the Indian Ocean is shown in Fig. 2. If the divergence of heat flux in a grid box is positive (negative), the ITF waters absorb (release) heat through diffusion, mixing or heat exchange in that grid box. Overall, ITF waters absorb heat in the northern Indian Ocean and release heat in the southern Indian Ocean, separated by approximate 12°S. In the northern Indian Ocean, there is a strong pattern of warming in entering region between 12°S and Java coast, the western boundary current region along Somalia coast, flank of the South Indian tropical gyre. The ITF waters in Route 4 seem to be responsible to this warming process. ITF wa-

ters upwell to surface layers and get warmer in northern Indian Ocean (Song et al., 2004; Valsala and Ikeda, 2007). In the southern Indian Ocean, cooling is confined to a broad band between 12°S and 18°S, the coastal current region along Africa coast, the eastern coast of Madagascar, and Leeuwin coast. The cooling along Leeuwin coast seems to associate with the ITF waters in Route 1, and the other cooling is contributed by the ITF waters in Routes 2, 3 and 4. Totally, the ITF waters release 0.56 PW heat, almost half of the heat entering the Indian Ocean, to the southern Indian Ocean during crossing this region. While the ITF waters absorb 0.41 PW heat from northern Indian Ocean. The heat gain compensates for the heat loss, resulting an “insignificant” net heat contribution, only 0.15 PW.

Shallow meridional overturning of the ITF waters in the Indian Ocean seems to be responsible for heat gain of the ITF waters in the northern Indian Ocean and heat loss in the southern Indian Ocean. This process could be diagnosed by the Lagrangian meridional streamfunction (Fig. 3). The ITF waters anticlockwise overturn in the northern Indian Ocean, mainly restrained in the upper 200 m (Fig. 3a). The ITF waters absorb heat within the overturning process in the northern Indian Ocean (Fig. 3b). The cool waters (most are less than 25°C) are heated mainly between 12°S and 5°N. After absorbing heat there, these waters return to the southern Indian Ocean with temperatures more than 27°C. This overturning process has a strength of $5 \times 10^6 \text{ m}^3/\text{s}$, about half of the total ITF volume transport. Overall, the ITF waters absorb heat from the northern Indian Ocean, implying that the ITF cools the northern Indian Ocean. In the southern Indian Ocean, the ITF waters cross the basin southward, residing in the upper 1 000 m (Fig. 3a). Within the poleward transport, most of the warm waters (more than 26°C) release heat, exiting the Indian Ocean with temperatures less than 25°C (Fig. 3b). Note that there is also an anticlockwise cell centered on 12°S, 26°C, with a strength of about $2 \times 10^6 \text{ m}^3/\text{s}$. This cell seemingly holds together with the overturning in the northern Indian Ocean. The waters in this cell firstly release heat to the southern Indian Ocean between 12°S and 22°S, then absorb heat within the overturning in the northern Indian Ocean, and finally re-release heat to the southern Indian Ocean. Overall, the ITF waters release heat to the southern Indian Ocean, indicating that the ITF warms the southern Indian Ocean.

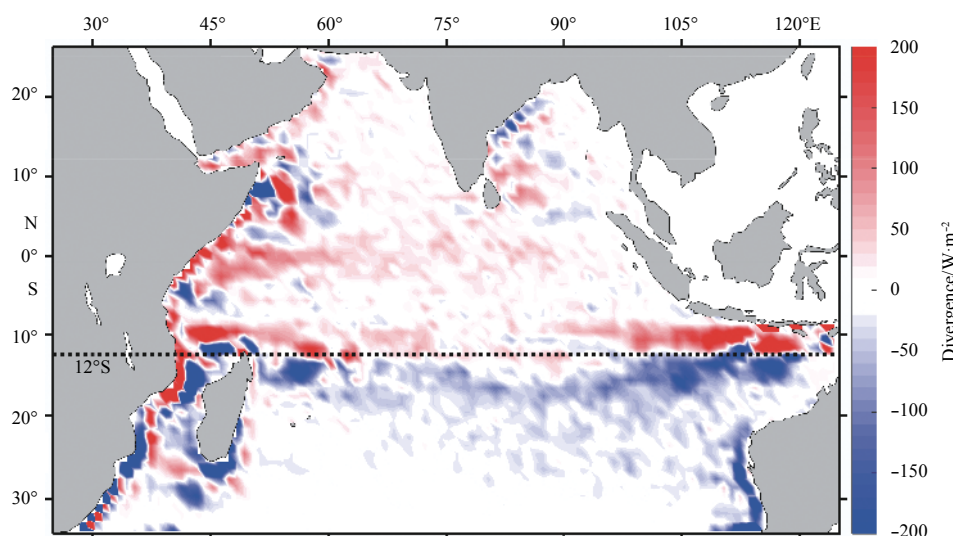


Fig. 2. The Lagrangian divergence of heat flux for ITF transporting in the Indian Ocean. The positive (negative) values indicate that ITF waters increase (decrease) temperature at that grid.

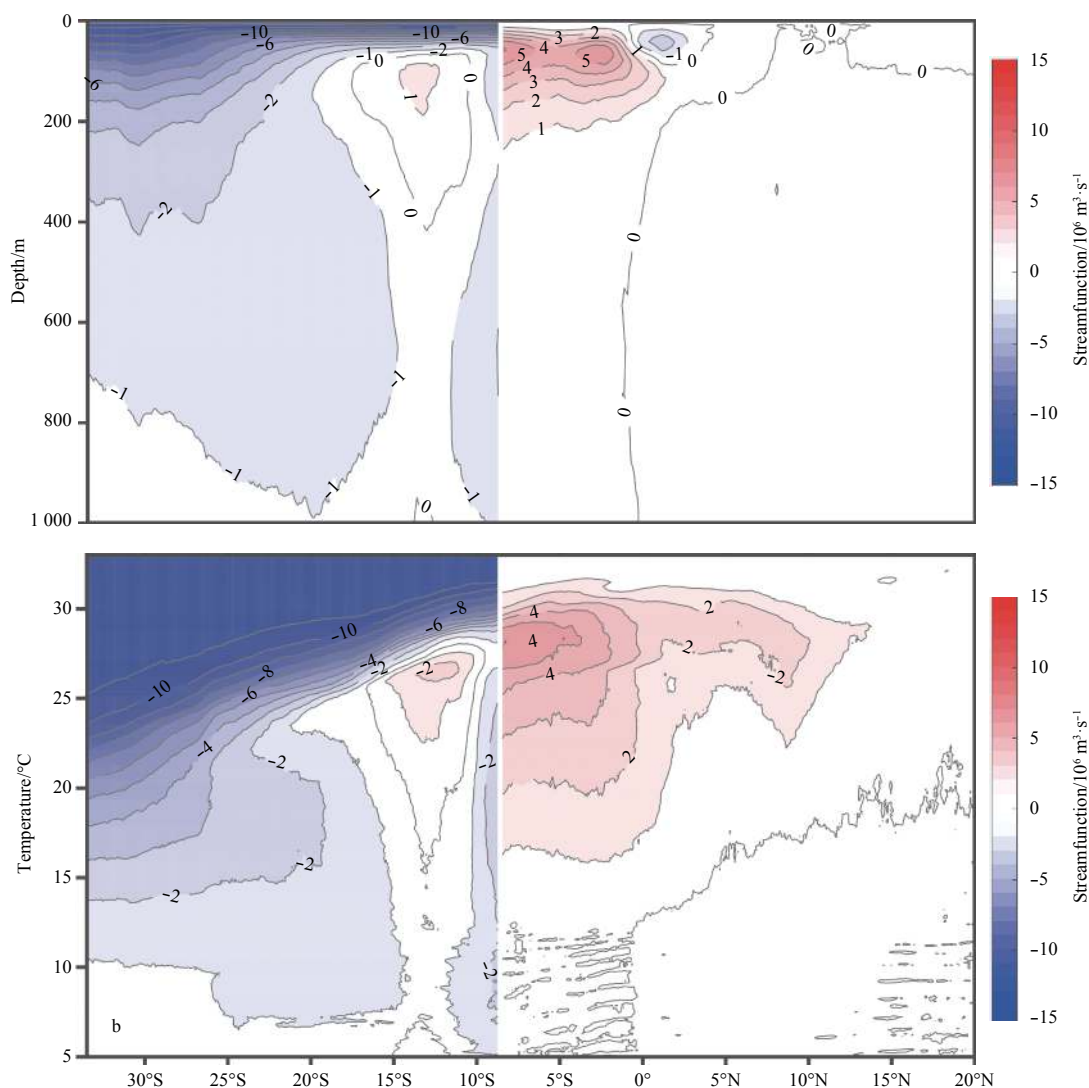


Fig. 3. The Lagrangian meridional overturning streamfunction in latitude-depth coordinates (a) and latitude-temperature coordinates (b). Positive streamlines correspond to anticlockwise circulation and negative streamlines to clockwise circulation.

3.3 Net heat contribution of ITF to the Indian Ocean

Furthermore, the exit of the ITF waters is carefully examined, in order to further estimate the net heat contribution of ITF transport to the Indian Ocean. Due to that the Indian Ocean has no high northern latitudes, the ITF waters have to leave at the southern boundary of the Indian Ocean. There are two main outflow regions (Wang et al., 2012), where the ITF waters exit the Indian Ocean. They are on both sides of ocean basin at the 34°S, in which one is within AC and the other is within LC (Fig. 4). Consistent with earlier studies (Haines et al., 1999; Song et al., 2004), they are estimated by 89% of ITF waters leaving within AC. These waters are mainly concentrated in the upper 1 500 m layers between the Africa coast and 30°E (see details in Fig. 4). The rest 11% leaving within LC mainly confined in the upper 200 m layers between 108°E and the Australia coast. These waters are nonnegligible in estimating the net heat contribution, as shown in latter section. The ITF waters in Route 1 leave the Indian Ocean within LC, and that in Routes 2, 3 and 4 eventually leave the Indian Ocean within AC.

From entrance section to exit section, most of the ITF waters get cooler and saltier (Fig. 5). At the entrance section, the inflow-

ing Pacific waters are converted by various mixing into a unique ITF waters stratification (Godfrey et al., 2007; Koch-Larrouy et al., 2008). For the ITF waters eventually exiting within LC, they mainly enter with high temperatures (more than 27°C) and low salinities (less than 34.5). While for the waters eventually exiting within AC, they enter with more widespread temperatures and salinities. At the exit section, the total distribution of the ITF waters has changed under interacting with the Indian Ocean waters (Vranes et al., 2002; Song et al., 2002). All the waters exiting within AC are less than 28°C while all that exiting within LC are less than 23°C. The waters are more concentrated on respective boundary current region, which are separated by higher salinities (more than 35.5) in LC region and relative lower salinities (but most still are more than 35.3) in AC region. Strong salinity modification and corresponding freshwater transport will be leaved to further research, and later we focus on the heat transport and the net heat contribution induced by temperature modification.

The heat transport and the net heat contribution in detail are given in Table 1. At entrance section, the total heat transport is about 1.04 PW, in which 0.89 PW is carried by the ITF waters exiting within AC and the rest 0.15 PW is carried by the ITF waters ex-

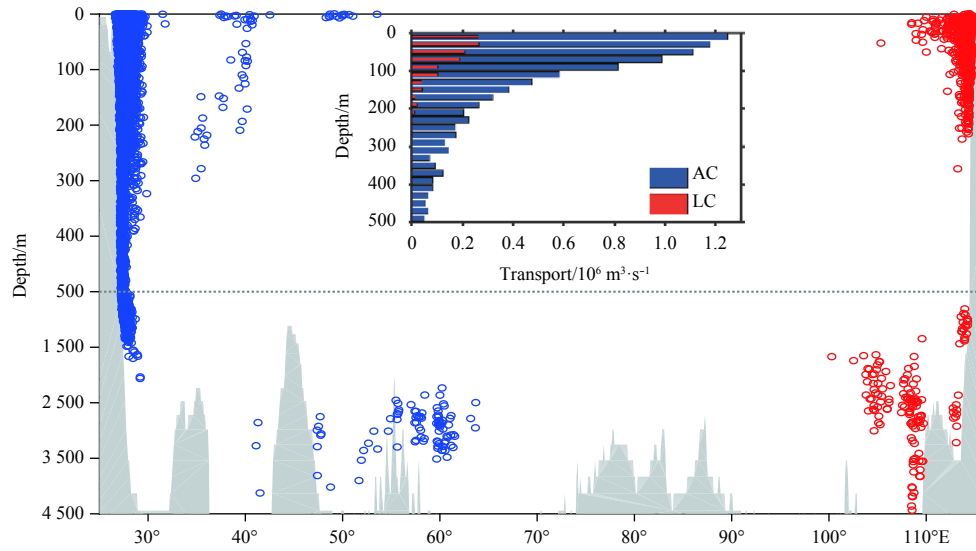


Fig. 4. The positions of the ITF waters exiting the Indian Ocean through the 34°S section. The symbol cycle represents the water exiting at that grid. The 500 m isobath is marked by gray dashed line. The waters exiting within AC and LC are respectively marked as blue and red, with the corresponding cumulative transport in 20 m depth bins are displayed by the bar graph in the upper of the panel.

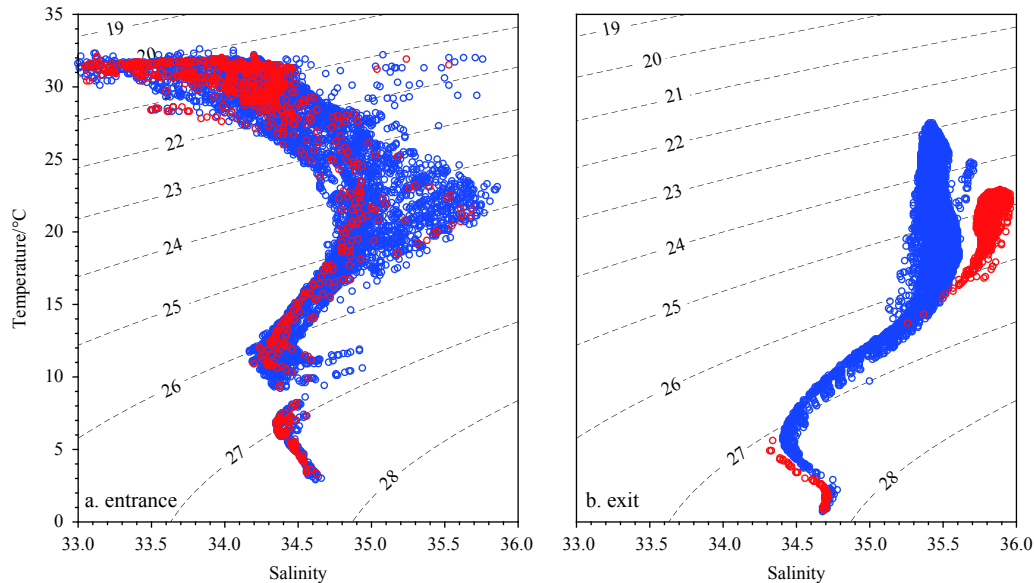


Fig. 5. TS diagram of the ITF waters at the entrance (8°S) (a) and the exit (34°S) (b). The waters exiting within AC and LC are marked as blue and red, respectively.

Table 1. Heat transport (PW, calculated following Eqs (4)–(6)) of the ITF waters at the entrance section, exit section and net heat contribution

	AC ⁺	AC ⁻	AC	LC	Total
Entrance	0.69	0.20	0.89	0.15	1.04
Exit	0.46	0.33	0.79	0.10	0.89
Net	0.23	-0.13	0.10	0.05	0.15

Note: The waters exiting within AC are further decomposed to AC⁺ and AC⁻, which are corresponding to the net heat loss and gain, respectively.

iting within LC. At exit section, the former reduces to 0.79 PW and the latter reduces to 0.10 PW, resulting the total heat transport reduces to 0.89 PW. In comparison of the heat transport between entrance section and exit section, the total net heat contribution

is 0.15 PW. This result is consistent with the eralier estimations (Banks, 2000; Vranes et al., 2002; Talley, 2003; Macdonald and Baringer, 2013). Although only 11% ITF waters exit within LC, due to that they all get cooler (Fig. 5), their net contribution is 0.05 PW, about 30% of total heat contribution. These waters flow in Route 1 and release heat within the poleward transport, which are nonnegligible in estimating the net heat contribution. For the ITF waters exiting within AC, a dominant part (AC⁺) get cooler while other considerable part (AC⁻) get warmer due to the over-turning process. The former have a net heat loss 0.23 PW while the latter have a net heat gain 0.13 PW, resulting their net heat contribution 0.10 PW. Due to the heat exchange compensation, the total net heat contribution of the ITF to the whole Indian Ocean is only 0.15 PW.

4 Conclusions and discussion

By using TRACMASS based on the high-resolution OFES data, the present study estimates the heat transport of the ITF waters in the Indian Ocean. The tracing reveals that the ITF waters flow westward and branch near Madagascar, further showing the ITF waters are redistributed in both northern and southern Indian Ocean. The ITF waters carry 1.04 PW heat into the Indian Ocean. This value is consistent with earlier estimations (Talley, 2003; Macdonald and Baringer, 2013). During the journey in the Indian Ocean, the ITF waters absorb 0.41 PW heat from the northern Indian Ocean while release 0.56 PW heat to the southern Indian Ocean. Due to this heat exchange compensation, the ITF waters have an “insignificant” net heat contribution to the whole Indian Ocean, only 0.15 PW. This indicates that the ITF cools the northern Indian Ocean while warms the southern Indian Ocean. Note that the northern Indian Ocean gains heat from atmosphere while the southern Indian Ocean releases heat to atmosphere (Yu et al., 2007; Liang and Yu, 2016), and therefore the ITF plays a critical role in heat budget in the Indian Ocean. Shallow meridional overturning of the ITF waters further indicates dynamic process responsible for heat gain of the ITF waters in the northern Indian Ocean and heat loss in the southern Indian Ocean. Through overturning process, the ITF waters absorb heat from the northern Indian Ocean due to the upwelling of the cold waters and release heat to the southern Indian Ocean with the poleward transport.

Furthermore, the tracing pathways show that 89% of the ITF waters exit the Indian Ocean within AC region, and the rest 11% exit within LC region. The former concentrate in the upper 1 500 m layers between the Africa coast and 30°E, and the latter are mainly confined in the upper 200 m layers between 108°E and the Australia coast. In comparison of the heat transport between entrance section and exit section, the ITF waters overall warm the Indian Ocean, with net heat contribution 0.15 PW. This result is consistent with the earlier estimations (Banks, 2000; Vranes et al., 2002; Talley, 2003; Macdonald and Baringer, 2013). Although only 11% ITF waters exit within LC region, they account for 0.05 PW, about 30% of total net heat contribution, which are neglected in the estimation by Vranes et al. (2002). For the ITF waters exiting within AC, a dominant part have a net heat loss 0.23 PW while the other have a net heat gain 0.13 PW, resulting their net heat contribution 0.10 PW.

In the present study, the trajectories are driven by monthly mean climatological velocity fields, which give a “mean” path. Since the dominant seasonal variability is included in the monthly climatology (Song et al., 2004), it is not unreasonable to regard the routes of ITF as a plausible estimate. The key transport process, a portion of the ITF waters flush into the northern Indian Ocean and absorb heat from there, has also been confirmed by earlier studies (Schott et al., 2002; Miyama et al., 2003; Song et al., 2004; Valsala and Ikeda, 2007). The main results of this paper, the ITF cools the northern Indian Ocean and warms the southern Indian Ocean, should be reliable. However, it has to be acknowledged that the tracing used in present study has limitations. The sub-grid motion is not represented in the trajectories. The sub-grid motion involving diffusion, mixing and turbulence affects spreading pathway in real ocean (Döös and Engqvist, 2007; Valsala and Ikeda, 2007). Future work needs to trace the ITF waters with adding sub-grid scale process and compare the results with that in the present paper.

Acknowledgements

We are grateful to the OFES group for providing the simula-

tion data publicly, and to the TRACMASS group for opening the tracing code.

References

- Banks H T. 2000. Indonesian Throughflow in a coupled climate model and the sensitivity of the heat budget and deep overturning. *Journal of Geophysical Research: Oceans*, 105(C11): 26135–26150, doi: [10.1029/1999JC000083](https://doi.org/10.1029/1999JC000083)
- Berglund S, Döös K, Nycander J. 2017. Lagrangian tracing of the water-mass transformations in the Atlantic Ocean. *Tellus A: Dynamic Meteorology and Oceanography*, 69(1): 1306311, doi: [10.1080/16000870.2017.1306311](https://doi.org/10.1080/16000870.2017.1306311)
- Domingues C M, Maltrud M E, Wijffels S E, et al. 2007. Simulated Lagrangian pathways between the Leeuwin Current System and the upper-ocean circulation of the southeast Indian Ocean. *Deep Sea Research Part II: Topical Studies in Oceanography*, 54(8–10): 797–817
- Döös K, Engqvist A. 2007. Assessment of water exchange between a discharge region and the open sea: a comparison of different methodological concepts. *Estuarine, Coastal and Shelf Science*, 74(4): 709–721, doi: [10.1016/j.ecss.2007.05.022](https://doi.org/10.1016/j.ecss.2007.05.022)
- Döös K, Kjellsson J, Jönsson B. 2013. TRACMASS-A Lagrangian trajectory model. In: Soomere T, Quak E, eds. *Preventive Methods for Coastal Protection*. London: Springer, 225–249
- Döös K, Nilsson J, Nycander J, et al. 2012. The world ocean thermohaline circulation. *Journal of Physical Oceanography*, 42(9): 1445–1460, doi: [10.1175/JPO-D-11-0163.1](https://doi.org/10.1175/JPO-D-11-0163.1)
- Godfrey J S. 1996. The effect of the Indonesian Throughflow on ocean circulation and heat exchange with the atmosphere: A review. *Journal of Geophysical Research: Oceans*, 101(C5): 12217–12237, doi: [10.1029/95JC03860](https://doi.org/10.1029/95JC03860)
- Godfrey J S, Hu Ruijin, Schiller A, et al. 2007. Explorations of the annual mean heat budget of the tropical Indian Ocean. Part I: studies with an idealized model. *Journal of Climate*, 20(13): 3210–3228, doi: [10.1175/JCLI4157.1](https://doi.org/10.1175/JCLI4157.1)
- Gordon A L. 1986. Inter-ocean exchange of thermocline water. *Journal of Geophysical Research: Oceans*, 91(C4): 5037–5046, doi: [10.1029/JC091iC04p05037](https://doi.org/10.1029/JC091iC04p05037)
- Gordon A L. 2005. Oceanography of the Indonesian seas and their throughflow. *Oceanography*, 18(4): 14–27, doi: [10.5670/oceanog](https://doi.org/10.5670/oceanog)
- Gordon A L, Sprintall J, Van Aken H M, et al. 2010. The Indonesian Throughflow during 2004–2006 as observed by the INSTANT program. *Dynamics of Atmospheres and Oceans*, 50(2): 115–128, doi: [10.1016/j.dynatmoce.2009.12.002](https://doi.org/10.1016/j.dynatmoce.2009.12.002)
- Haines M A, Fine R A, Luther M E, et al. 1999. Particle trajectories in an Indian Ocean model and sensitivity to seasonal forcing. *Journal of Physical Oceanography*, 29(4): 584–598, doi: [10.1175/1520-0485\(1999\)029<0584:PTIAIO>2.0.CO;2](https://doi.org/10.1175/1520-0485(1999)029<0584:PTIAIO>2.0.CO;2)
- Hu Ruijin, Godfrey J S. 2007. Explorations of the annual mean heat budget of the tropical Indian Ocean. Part II: studies with a simplified ocean general circulation model. *Journal of Climate*, 20(13): 3229–3248, doi: [10.1175/JCLI4158.1](https://doi.org/10.1175/JCLI4158.1)
- Kajtar J B, Santoso A, England M H, et al. 2015. Indo-Pacific climate interactions in the absence of an Indonesian Throughflow. *Journal of Climate*, 28(13): 5017–5029, doi: [10.1175/JCLI-D-14-00114.1](https://doi.org/10.1175/JCLI-D-14-00114.1)
- Koch-Larrouy A, Madec G, Blanke B, et al. 2008. Water mass transformation along the Indonesian Throughflow in an OGCM. *Ocean Dynamics*, 58(3–4): 289–309
- Lee T, Awaji T, Balmaseda M, et al. 2010. Consistency and fidelity of Indonesian-Throughflow total volume transport estimated by 14 ocean data assimilation products. *Dynamics of Atmospheres and Oceans*, 50(2): 201–223, doi: [10.1016/j.dynatmoce.2009.12.004](https://doi.org/10.1016/j.dynatmoce.2009.12.004)
- Lee T, Fukumori I, Menemenlis D, et al. 2002. Effects of the Indonesian Throughflow on the Pacific and Indian oceans. *Journal of Physical Oceanography*, 32(5): 1404–1429, doi: [10.1175/1520-0485\(2002\)032<1404:EOTITO>2.0.CO;2](https://doi.org/10.1175/1520-0485(2002)032<1404:EOTITO>2.0.CO;2)
- Liang Xinfeng, Yu Lisan. 2016. Variations of the global net air-sea

- heat flux during the “hiatus” period (2001–10). *Journal of Climate*, 29(10): 3647–3660, doi: [10.1175/JCLI-D-15-0626.1](https://doi.org/10.1175/JCLI-D-15-0626.1)
- Lumpkin R, Speer K. 2007. Global ocean meridional overturning. *Journal of Physical Oceanography*, 37(10): 2550–2562, doi: [10.1175/JPO3130.1](https://doi.org/10.1175/JPO3130.1)
- Macdonald A M, Baringer M O. 2013. Ocean heat transport. In: Siedler G, Griffies S, Gould J, eds. *Ocean Circulation and Climate: A 21st Century Perspective*. 2nd ed. Oxford: Academic Press, 759–785
- Masumoto Y. 2010. Sharing the results of a high-resolution ocean general circulation model under a multi-discipline framework—a review of OFES activities. *Ocean Dynamics*, 60(3): 633–652, doi: [10.1007/s10236-010-0297-z](https://doi.org/10.1007/s10236-010-0297-z)
- Masumoto Y, Morioka Y, Sasaki H. 2008. High-resolution Indian ocean simulations—recent advances and issues from OFES. In: Hecht M W, Hasumi H, eds. *Ocean Modeling in an Eddy Regime*. Washington, DC: AGU, 199–212
- Masumoto Y, Sasaki H, Kagimoto T, et al. 2004. A fifty-year eddy-resolving simulation of the world ocean—Preliminary outcomes of OFES (OGCM for the Earth Simulator). *Journal of the Earth Simulator*, 1: 35–56
- McCreary J P, Miyama T, Furue R, et al. 2007. Interactions between the Indonesian Throughflow and circulations in the Indian and Pacific Oceans. *Progress in Oceanography*, 75(1): 70–114, doi: [10.1016/j.pocean.2007.05.004](https://doi.org/10.1016/j.pocean.2007.05.004)
- Metzger E J, Hurlburt H E, Xu X, et al. 2010. Simulated and observed circulation in the Indonesian Seas: 1/12° global HYCOM and the INSTANT observations. *Dynamics of Atmospheres and Oceans*, 50(2): 275–300, doi: [10.1016/j.dynatmoce.2010.04.002](https://doi.org/10.1016/j.dynatmoce.2010.04.002)
- Miyama T, McCreary J P, Jensen T G, et al. 2003. Structure and dynamics of the Indian-Ocean cross-equatorial cell. *Deep Sea Research Part II: Topical Studies in Oceanography*, 50(12–13): 2023–2047
- Schott F A, Dengler M, Schoenfeldt R. 2002. The shallow overturning circulation of the Indian Ocean. *Progress in Oceanography*, 53(1): 57–103, doi: [10.1016/S0079-6611\(02\)00039-3](https://doi.org/10.1016/S0079-6611(02)00039-3)
- Seville E, Sprintall J, Schwarzkopf F U, et al. 2014. Pacific-to-Indian ocean connectivity: Tasman leakage, Indonesian throughflow, and the role of ENSO. *Journal of Geophysical Research: Oceans*, 119(2): 1365–1382, doi: [10.1002/2013JC009525](https://doi.org/10.1002/2013JC009525)
- Song Q, Gordon A L, Visbeck M. 2004. Spreading of the Indonesian throughflow in the Indian Ocean. *Journal of Physical Oceanography*, 34(4): 772–792, doi: [10.1175/1520-0485\(2004\)034<0772:SOTITI>2.0.CO;2](https://doi.org/10.1175/1520-0485(2004)034<0772:SOTITI>2.0.CO;2)
- Song Qian, Vecchi G A, Rosati A J. 2007. The role of the Indonesian Throughflow in the Indo-Pacific climate variability in the GF-DL coupled climate model. *Journal of Climate*, 20(11): 2434–2451, doi: [10.1175/JCLI4133.1](https://doi.org/10.1175/JCLI4133.1)
- Sprintall J, Gordon A L, Koch-Larrouy A, et al. 2014. The Indonesian seas and their role in the coupled ocean-climate system. *Nature Geoscience*, 7(7): 487–492, doi: [10.1038/ngeo2188](https://doi.org/10.1038/ngeo2188)
- Sprintall J, Wijffels S, Gordon A L, et al. 2004. INSTANT: A new international array to measure the Indonesian Throughflow. *EOS, Transactions American Geophysical Union*, 85(39): 369–376
- Talley L D. 2003. Shallow, intermediate, and deep overturning components of the global heat budget. *Journal of Physical Oceanography*, 33(3): 530–560, doi: [10.1175/1520-0485\(2003\)033<0530:SIADOC>2.0.CO;2](https://doi.org/10.1175/1520-0485(2003)033<0530:SIADOC>2.0.CO;2)
- Talley L D. 2008. Freshwater transport estimates and the global overturning circulation: Shallow, deep and throughflow components. *Progress in Oceanography*, 78(4): 257–303, doi: [10.1016/j.pocean.2008.05.001](https://doi.org/10.1016/j.pocean.2008.05.001)
- Valsala V K, Ikeda M. 2007. Pathways and effects of the Indonesian Throughflow water in the Indian Ocean using particle trajectory and tracers in an OGCM. *Journal of Climate*, 20(13): 2994–3017, doi: [10.1175/JCLI4167.1](https://doi.org/10.1175/JCLI4167.1)
- Vranes K, Gordon A L, Field A. 2002. The heat transport of the Indonesian Throughflow and implications for the Indian Ocean heat budget. *Deep Sea Research Part II: Topical Studies in Oceanography*, 49(7–8): 1391–1410
- Wajsowicz R. 2002. Air-sea interaction over the Indian Ocean due to variations in the Indonesian Throughflow. *Climate Dynamics*, 18(5): 437–453, doi: [10.1007/s00382-001-0187-7](https://doi.org/10.1007/s00382-001-0187-7)
- Wang Weiqiang, Köhl A, Stammer D. 2010. Estimates of global ocean volume transports during 1960 through 2001. *Geophysical Research Letters*, 37(15): L15601
- Wang Weiqiang, Köhl A, Stammer D. 2012. The deep meridional overturning circulation in the Indian Ocean inferred from the GECCO synthesis. *Dynamics of Atmospheres and Oceans*, 58: 44–61, doi: [10.1016/j.dynatmoce.2012.08.001](https://doi.org/10.1016/j.dynatmoce.2012.08.001)
- Yu Lisan, Jin Xiangze, Weller R A. 2007. Annual, seasonal, and inter-annual variability of air-sea heat fluxes in the Indian Ocean. *Journal of Climate*, 20(13): 3190–3209, doi: [10.1175/JCLI4163.1](https://doi.org/10.1175/JCLI4163.1)
- Zika J D, England M H, Sijp W P. 2012. The ocean circulation in thermohaline coordinates. *Journal of Physical Oceanography*, 42(5): 708–724, doi: [10.1175/JPO-D-11-0139.1](https://doi.org/10.1175/JPO-D-11-0139.1)